A Novel Ka-band Spatial Combiner Amplifier: Global Design and Modeling

Alberto Leggieri[1], **Davide Passi**[1], **Franco Di Paolo**[1], **Marco Bartocci**[2], **Antonio Tafuto**[2], **and Antonio Manna**[2]

[1]Department of Electronic Engineering, University of Rome Tor Vergata, Rome, Italy
[2]Elettronica SpA, Via Tiburtina Valeria Km. 13, Rome 7-00100, Italy

Abstract— This article describes the complete design of high performances Ka-Band small size Spatial Power Combiner (SPC) Amplifier. Several multiple physics aspects are treated in the proposed study as electromagnetic behavior and thermo-mechanical features. The combiner consists of quadruple Fin lines to microstrip (FLuS) transitions inserted into a WR28 waveguide T-junction. In this structure, 16 Monolithic Microwave Integrated Circuit (MMIC) Solid State Power Amplifiers (SSPA's) are integrated. In order to drive the active devices at full power, thermal exposition has been controlled by an opportune heat-sinker subjected to a cooling air flow. A main design has been followed by FEM simulation using Ansys-Ansoft HFSS and Comsol Multiphysics. Scattering parameters, stresses and strains have been computed together with the temperature and airflow distributions. A mean insertion loss of 2 dB is achieved with a return loss better the 10 dB in the 31–37 GHz bandwidth while operating at maximum power. In such condition, the transistors present a maximum displacement of 28.7 μm caused by the thermal expansion of the material due to a channel temperature of 125°C, and special techniques have to been applied to avoid the MMIC's breakage.

1. INTRODUCTION

Spatial Power Combiner (SPC) Technology [1–7] is actually knowing an increasing interest as a suitable alternative to high power Vacuum Tubes (VT's) microwave amplification. A single VT has higher power output than a single transistor but the reliability and low voltage operation [8, 9] of the Solid State (SS) technology may give a notable benefit. Of course, in the range of millimeter waves and signal power levels greater than kilowatt only VT's like Gyrotrons or Free Electron Lasers can be employed [10–13], and no competition exists between SSPA's and VT's. The traditional approach to obtain a significant power output using SSPA's is the binary combining of many transistors through microstrip Transmission Lines [14, 15]. This solution is limited to the losses which each printed transmission line (TL) combiner and to the limited number of devices to a power of two. The Spatial Power Combining approach shows evident advantages over the classical binary technique. This technique is employed to design the Spatial Power Amplifier (SPA), in which power dividing and combining is performed in a parallel way, rather than in a serial way, and losses are little dependent with the number of used PA's [16]. Furthermore, SPA loss is rather constant with the number of amplifiers. In this work, the design and simulation a novel high performance and small size SPC working in Ka Band is presented, interfacing with standard WR28 waveguides. It employs an innovative matched quadruple antipodal Fin Line transition. Such innovative SPC allows the in-phase combination of 16 MMIC PA's achieving a high combining efficiency. Several circuital and technological solutions have been adopted [17]. In order to reduce the combining loss and size and to reach wideband matching, exponential Finline-to-microstrips (FLuS) transitions have been considered. In order to improve the operative band, a parasitic void has been implemented by inserting an anti-resonance metal in the antipodal FLuS transition profile [18]. Together with the electromagnetic (EM) design of the SPA, the whole structure has been developed for the corrected thermo-mechanical operation which ensures the desired electromagnetic behavior, and avoids undesired alteration due to the thermo-mechanical effects related to the operative condition of the devices.

When high power levels are manipulated, heat sinking systems are especially important in order to avoid performance degradation and even device failure [19]. The power dissipation of the active devices produces a considerable temperature increase of both the PA's and the connected structure. If the SSPA's temperature exceeds the maximum allowed value (specified by the SSPA's vendor), an amplification failure or device damage may occur. The computation of the temperature is performed when the heat generated by the MMIC's power dissipation has been diffused on all the reachable SPA components which have been cooled by the opportune heat sinkers connected to the device body cooled by an incident air flow. The calculation is performed through a stationary analysis when the system is thermally stable. A fixed external temperature has been assumed for the inlet air particles. The heat exchange occurs over all the SPA outer surfaces but is maximized on the heat sinker structure. A Finite Element Method (FEM) based simulation using Ansys-Ansoft HFSS has been employed to predict the Electromagnetic behavior of the structure and a Multiphysics modeling based design using COMSOL has been employed to perform Thermodynamics and Fluid-Dynamics analysis coupled to structural mechanics computation. Stresses and strains have been computed together with the temperature and airflow distributions. In order to decrease computational time and resources while maintaining accuracy and a nice grade of reliability, the device model is organized by using several architectural strategies shown in this paper. Since the device has two symmetry planes, only a quarter of the SPC structure has been employed for the modeling by introducing opportune symmetry boundary conditions.

2. ELECTROMAGNETIC DESIGN

The amplifier reported in this paper uses a WR28 rectangular waveguide at input and output. In order to deliver power to MMICs, four Al_2O_3 cards were employed, each one containing quadruple (quad) FLuS transitions (Figure 1). The Fin Line taper in each FLuS can be used as a broad-band impedance transformer between the waveguide and MMIC amplifier. To reduce the combining loss, an exponential FL taper has been chosen in antipodal configuration [20]:

$$w(z) = w_0 \exp\left[\frac{z}{l}\ln(w_f)\right], \tag{1}$$

where w_0 stands for initial taper width, w_f for the final one and l is the total length of the transition. It can be demonstrated that the impedance vary with the same behavior of (1) [21]. Microstrip Lines were designed following Hammerstad formulas reported in [22]. To improve the return loss at the waveguide when loaded by the Fin Lines and to symmetrise currents on the substrate, dielectric Parallel Quarter Wave Transformers (P-QWT's) have been designed, starting by the general design philosophy for single QWT given in [20].

The selection of the simulated geometry has been carefully determined, to avoid undesired lack of software convergence or bad results [23]. The 3D simulated structure is shown in Figure 2, from which we recognize that one quarter of the structure shown in Figure 2 can be analyzed with the software. The wave equation in the frequency domain (2) has been solved by HFSS Driven Modal

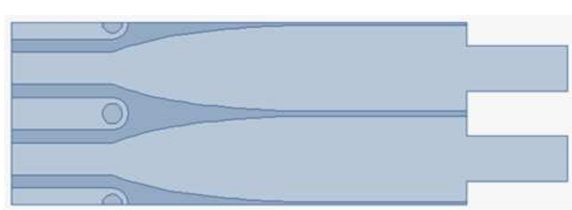

Figure 1: Quadruple FLuS employing the innovative dielectric parallel QWT.

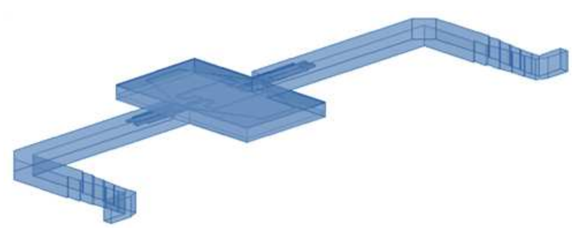

Figure 2: 3D quarter section of the WR28 SPC EM model.

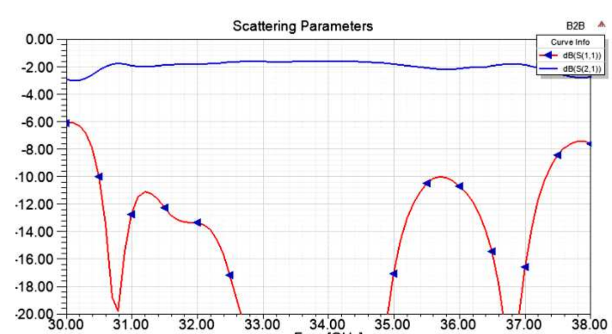

Figure 3: SPC simulation results: insertion loss and return loss in dB, in the operating bandwidth.

computation [19].

$$\nabla \times \mu_r^{-1} \left(\nabla \times \bar{E}\right) - k_0^2 \left(\varepsilon_r - \frac{j\sigma}{\omega\varepsilon_0}\right) \bar{E} = 0 \tag{2}$$

where μ_r is the permeability, ε_r the permittivity and σ the conductivity of the material; ε_0 is the permittivity of the vacuum, k_0 the wave number in free space, ω the wave angular frequency and $\bar{E}$ the electric field. The simulated S-parameters are given in Figure 3. By observing such images we note that the proposed WR28 SPC passive structure ensures a maximum insertion loss of 2.2 dB and a minimum Return Loss of 10 dB in the whole 31–37 GHz band.

3. THERMO-MECHANICAL DESIGN

The heat generated by power dissipation on the MMIC's channel cause carriers and shell warming. If no cooling system is provided the SPA's temperature increase until the active devices breakdown. For this reason, an opportune cooling system has been designed formed by heat sinks and cooling fan. The analyzed structure is realized in a WR28 waveguide, whose central part allows for the insertion of two metal carrier which holds up the antipodal FLuS's and MMIC SSPA's. The material to use for the carrier has been investigated in this work, in order to improve the heat conduction. An Aluminum shell contains two 2 mm copper carriers. The carriers are placed at the center of the waveguide and each face of the carrier holds 8 active devices and 2 FLuS's printed on an Alumina substrate. The model used for the analysis is shown in Figure 4. The heat sources are 16 parallelepipeds, one per MMIC, with size of $5.4 \times 0.2 \times 0.01$ mm; they represent the FET's channel and each source dissipate 21 W on GaAs. The analysis is based on the complete coupling of the COMSOL Laminar Flow, Heat Transfer and Structural Mechanics modules. No mechanical movements are allowed on the external walls, since has been assumed that the air can't move any part of the structure, including the heat-sinker wings. This condition avoids any normal force on the surfaces and any rotation, allowing for the computation of the sole heat exchange.

The Thermodynamics and fluid dynamics study has been solved by adopting a fully coupled stationary calculation in order to evaluate the temperature distribution, when the maximum temperature is reached by the active devices and all the structure is subjected to an opportune air flow.

Heat Transfer has been computed by solving the Heat Equation in the steady state (3) [24].

$$-\nabla \cdot (k\nabla T) = Q \tag{3}$$

where T is the temperature (K), k the thermal conductivity ($\mathrm{W{\cdot}m^{-1}{\cdot}K^{-1}}$) of the material and Q is the heat power density ($\mathrm{Wm^{-3}}$). The air motion is modeled with a single phase laminar flow and computed by solving the system of (4) and (5) in a stationary analysis.

$$\rho(u \cdot \nabla)u = \nabla \cdot \left[-pI + \mu\left(\nabla u + (\nabla u)^T\right) - \frac{2}{3}\mu\left(\nabla \cdot u\right) I\right] + F \tag{4}$$

$$\nabla \cdot (\rho u) = 0 \tag{5}$$

where p is the pressure, u is the velocity field ($\mathrm{m{\cdot}s^{-1}}$), ρ the material density ($\mathrm{kg{\cdot}m^{-3}}$), μ the dynamic viscosity (Pa·s) of the material (the air) and F is the volume force ($\mathrm{N{\cdot}m^{-3}}$). The symbol I stand for the identity matrix and T for the transposing operation.

The Structural Mechanics analysis shares the computation variables with the thermodynamic and fluid dynamics calculation, consisting in a large computation system. The thermal expansion calculated by the structural analysis has been employed to estimate the deformation of the material induced by the heat generated by the SSPA's power dissipation during the operation at the maximum power rating. Surfaces are intended as in a stationary temperature regime, cooled by the external environment condition as shown by the Thermo-Fluid Dynamics analysis. The analysis has solved the system of stress steady state Equation (6) fully coupled with the computation of the (3), (4) and (5) by computing the thermal expansion of the materials [19].

$$-\nabla \cdot \sigma = \bar{F}_V \tag{6}$$

where σ is the stress ($\mathrm{Nm^{-2}}$) and $\bar{F}_V$ is the force per unit volume ($\mathrm{Nm^{-3}}$). The mechanical boundary conditions have been chosen in order to leave waveguide external walls free from any constriction, ensuring the ability to swell. This condition avoids any normal force on such walls and any rotation, allowing to compute the complete deformation of the transistors. The solid model is intended as isotropic and the structural transient behavior as quasi-static. The thermal expansion induced forces have symmetric application points, due to the geometric symmetry. The surfaces which lie on the back plane of Figure 4 are modeled as symmetry boundary condition. The mechanical analysis has been performed by considering the nominal operative ratings of the SPC, while operating at maximum power of 21 W per transistor and cooling the SPC by an air laminar flux with a velocity of 10 ms and initial temperature of 0°C. This is a value obtainable with a liquid chiller or much easier when the SPC is employed on Airplanes. In the following images, black color outlines represent the original conformation, and the stained volumes represent the deformed structure. Furthermore, the scale factor of the deformation has been magnified, in order to better view the displacements. In Fig. 4 the airflow streamline is reported including the temperature distribution of the air flowing around the SPC structure. By the heat transfer with the warmed SPA, the air flux reaches a maximum temperature of 54.5°C. In such condition, the channels of the transistors reach a maximum temperature of 125°C shown in Fig. 5. In Fig. 6 is represented the maximum stress on the carrier and MMIC devices: it is located near the inner angles of the carrier and locally reaches 0.26 GNm^{-2}. MMIC devices need to be carefully held to the carrier since the different thermal expansion coefficients of the materials may induce a mismatch which can damage the crystal. A deep description of the physical principle governing these effects is reported in [26–29]. According to such studies and basing on our heritage by considering the stress to which the MMIC devices are subjected, a typical acceptable value for the displacement of a GaAs crystal of the dimensions of the employed MMIC, exactly the type TGA2575 produced by Triquint [30], needs to not exceed 5 µm on the narrow side. A maximum displacement of 56.3 µm is located on the cooling wings of the heat sinker and near the interface between the outermost SSPA's and the external surface of the SPC, is located a displacement of 28.7 µm (shown in Fig. 7), enough negligible from the EM guiding properties of the structure but critical for the GaAs MMIC survivability. In order to allow for the heat dissipation without mismatch between coefficients of thermal expansion (CTE) for GaAs and conductors, MMIC's are brazed onto CuMo heat spreader and the whole assembly is brazed onto copper carriers. Hence, at each temperature value obtained

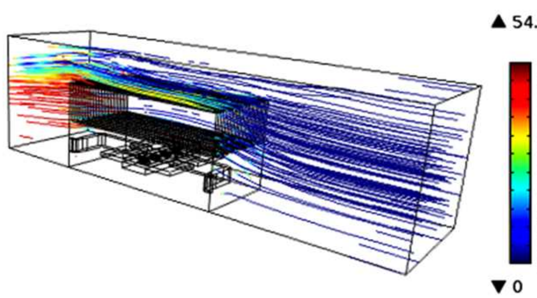

Figure 4: Airflow streamlines with temperature distribution on a quarter section of the SPC.

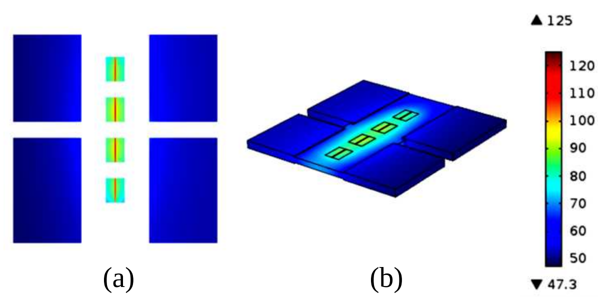

Figure 5: (a) Temperature distribution (°C) on carrier and MMIC in plane section and (b) 3D view.

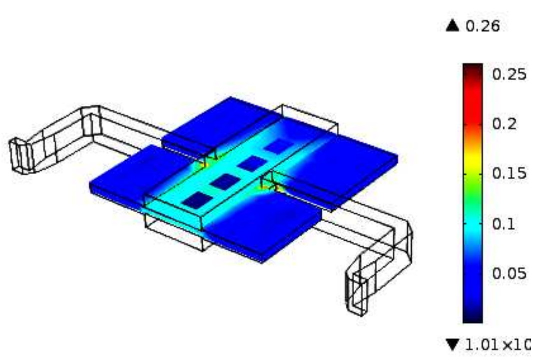

Figure 6: Maximum stress on carrier and MMIC (GNm^{-2}).

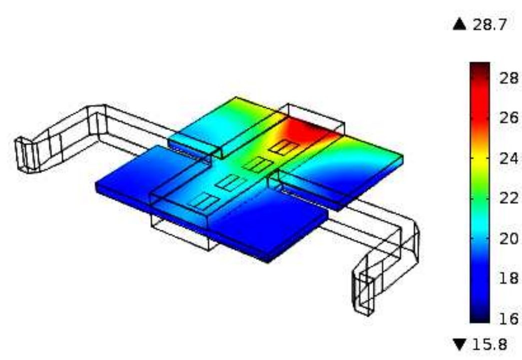

Figure 7: Maximum displacement on MMIC (µm).

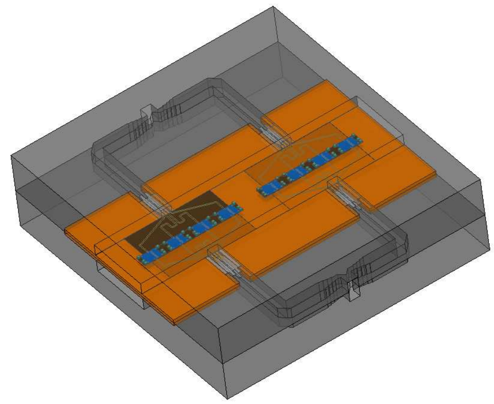

Figure 8: The whole structure of the Ka-band SPC amplifier.

we need to add about 4°C, by our heritage, to consider the CuMo effect in thermal conduction.

The mechanical design considers the compactness of the final SPA, the maximum possible heat transfer and the simplicity of the assembling. This SPA has been designed to use standard WR28 flanges and to employ 16 MMIC Triquint TGA2575 HPA's operating at these WG frequencies. At the amplifier input, a Waveguide T-junctions in E-plane is used to split the signals in two WR28 arms. The branches of T-junction have designed with four-step Chebyshev transformer in order to obtain small reflections to the input port in Ka band. In Figure 8 we report the complete CAD drawing of the Ka-band SPC amplifier, including 16 SSPA MMIC's: heat sinker is removed for a better view. From such image we recognize the bulk of the SPC made of Aluminum, the innovative quadruple fin lines with the innovative P-QWT, the copper carriers, the equalization lines and the MMIC's with their DC feed capacitors placed on CuMo heat spreader. The size of this SPC is $90 \times 92 \times 25$ mm, but size can be still reduced.

4. CONCLUSIONS

This study describes a novel SPC Ka Band Power Amplifier based on the spatial combination of 16 SSPA MMIC's. Several multiple physics aspects are treated in the proposed study as the electromagnetic behavior and thermo-mechanical features in order to drive the active devices at full power. A reliable computational electromagnetic model have shown an operating bandwidth from 31 GHz to 37 GHz, with a mean insertion loss of 2 dB for the passive SPC and minimum return loss of 10 dB in the whole bandwidth. MMICs fault and undesired thermal expansion with related stresses and displacements have been prevented. A maximum channel temperature of 125°C is expected while the device operates at full power and cooled by an opportune airflow. Maximum stress on the carriers, MMIC devices and cooling wings has been computed. Such a study has allowed for the selection of the proper materials for carriers and interfaces between them and MMIC's. Due to the proposed thermo-mechanical design, each MMIC device can be driven at full power reaching its maximum power output $P_{out} = 35.5$ dBm. Since the average Insertion Losses are 2.0 dB, the proposed SPA (employing 16 MMIC amplifiers) can provide a maximum power output of about 45.8 dBm occupying $90 \times 92 \times 25$ mm.

REFERENCES

1. Leggieri, A., G. Orengo, D. Passi, and F. Di Paolo, "The squarax spatial power combiner," *Progress In Electromagnetics Research C*, Vol. 45, 43–55, 2013.
2. Russo, I., L. Boccia, G. Amendola, and G. Di Massa, "Parametric analysis of grid amplifiers," *Proceedings of European Microwave Week*, 1326–1329, Amsterdam, 2008.
3. An, D., X. Li, J. Mou, and X. Liv, "A new type of Ka-band waveguide-based power combining structures," *Proceedings of ICMMT 2008*, 1–4, Nanjing, China, Apr. 21–24, 2008.
4. Russo, I., L. Boccia, G. Amendola, and H. Shumacher, "Compact hybrid coaxial achitecture for 3–10 GHz UWB quasi-optical power combiner," *Progress In Electromagnetics Research*, Vol. 122, 77–92, 2012.
5. Lopz, D., L. Bortoli, J-P Fraysse, D. Langrez, J. F. Villemazet, J. L. Cazaux, G. Soubercaze-Pun, and L. Lapierre, "HPA module for active antenna applications," *Proceedings of 5th European Microwave Integrated Circuit Conference*, 404–407, Paris, Sep. 27–28, 2010.

6. Jia, P., L. Y. Chen, A. Alexanian, and R. A. York, "Multioctave spatial power combining in oversized coaxial waveguide," *IEEE Trans. on MTT*, Vol. 50, No. 5, 1355–1360, May 2002.
7. Cheng, N.-S., P. Jia, D. B. Rensch, and R. A. York, "A 120-W X-band spatially combined solid-state amplifier," *IEEE Trans. on MTT*, Vol. 47, No. 12, 2557–2561, Dec. 1999.
8. Symons, R. S., "Tubes: Still vital after all these years," *IEEE Spectrum*, 52–63, Apr. 1998.
9. Barbour, E., "The cool sound of tubes," *IEEE Spectrum*, 24–35, Aug. 1998.
10. Levush, B., D. K. Abe, J. P. Calame, B. G. Danly, K. T. Nguyen, E. J. Dutkowski, R. H. Abrams, and R. K. Parker, "Vacuum electronics: Status and trends," *IEEE Radar Conference*, 971–976, 2007.
11. Armstrong, C. M., "The vitality of vacuum electronics," *IEEE 14th International Vacuum Electronics Conference (IVEC)*, 1–3, 2013.
12. Booske, J. H., R. J. Dobbs, C. D. Joye, C. L. Kory, G. R. Neil, G.-S. Park, J. Park, and R. J. Temkin, "Vacuum electronic high power terahertz sources," *IEEE Transactions on Terahertz Science and Technology*, Vol. 1, No. 1, 54–75, 2011.
13. Qiu, J. X., B. Levush, J. Pasour, A. Katz, C. M. Armstrong, D. R. Whaley, J. Tucek, K. Kreischer, and D. Gallagher, "Vacuum tube amplifiers," *IEEE Microwave Magazine*, Vol. 10, No. 7, 38–51, 2009.
14. Russel, K. J., "Microwave power combining techniques," *IEEE Trans. on MTT*, Vol. 27, No. 5, 472–478, May 1979.
15. Chang, K. and C. Sun, "Millimeter-wave power combining techniques," *IEEE Trans. on MTT*, Vol. 31, No. 2, 91–107, Feb. 1983.
16. DeLisio, M. P. and R. A. York, "Quasi-optical and spatial power combining," *IEEE Trans. on MTT*, Vol. 50, No. 3, Mar. 2002.
17. Passi, D., A. Leggieri, F. Di Paolo, M. Bartocci, A. Tafuto, and A. Manna, "High efficiency Ka-band spatial combiner," *Advanced Electromagnetics*, Vol. 3, No. 2, 10–15, 2014.
18. Ponchak, G. E. and A. N. Downey, "A new model for broadband waveguide to microstrip transition design," NASA Technical Memorandum 88905, Lewis Research Center Cleveland, Ohio, Dec. 1986.
19. Leggieri, A., D. Passi, F. Di Paolo, and G. Saggio, "Multiphysics design of a spatial combiner predisposed for thermo-mechanically affected operation," *Journal of Electromagnetic Waves and Applications*, Vol. 28, No. 17, 2153–2168, 2014.
20. Bhat, B. and S. K. Koul, *Analysis, Design and Applications of Fin Lines*, Artech House, 1987.
21. Collin, R. E., *Foundations for Microwave Engineering*, McGraw-Hill International Editions, 1992, ISBN 0-07-011811-6.
22. Di Paolo, F., *Networks and Devices Using Planar Transmission Lines*, CRC Press LLC, 2000, ISBN 0-8493-1835-1.
23. Passi, D., A. Leggieri, and F. Di Paolo, "Computational electromagnetic design of the squarax spatial power combiner," *Ansys UGM 2014*, Milano, Italy, 2014.
24. COMSOL "Heat transfer module user's guide," 75–99, 184–224, COMSOL AB, Stockholm, 2012,
25. COMSOL "Heat transfer module user's guide," 69–72; 111–212, COMSOL AB, Stockholm, 2012.
26. Chen, C. P., "Fracture MEchanics evaluation of GaAs," *JPL Report*, Oct. 15, 1984.
27. Vidano, R. P., D. W. Paananen, T. H. Miers, J. M. Krause-Singh, K. R. Agricola, and R. L. Hauser, "Mechanical stress reliability factors for packaging GaAs MMIC and LSIC components," *IEEE Trans. on Components, Hybrids, and Manufacturing Tech.*, No. 4, 612–617, Dec. 1987.
28. Pavio, J. and D. Hyde, "Effects of coefficient of thermal expansion mismatch on solder attached GaAs MMICs," *IEEE MTT-S International Microwave Symposium Digest*, Vol. 3, 1075–1078, 1991.
29. Jin, M., J. Xu, and Y. Fang, "Investigation on mechanical characteristics of semi-insulating GaAs crystal under different load," *International Conference on Materials for Renewable Energy & Environment (ICMREE)*, Vol. 1, 100–103, 2011.
30. Tryquint Semiconductor Inc., "TGA2575 Ka-band 3 watt power amplifier," Product Datasheet, 2012.